than one binding site is involved in the binding of I to bovine serum albumin (Fig. 4). The binding results obtained using the electrochemical method compare very well with those obtained using equilibrium dialysis and ultrafiltration (Fig. 4). However, results utilizing the rotating-disk technique can be obtained in a much shorter time and with considerably smaller amounts of materials.

Competive Binding between II and I—The observation made by Witiak *et al.* (10), indicating an unusual binding of I to rat serum albumin in the presence of low concentrations of II, was reinvestigated using both this electrochemical method and ultrafiltration. The spectrophotometric results in the Witiak *et al.* study could be interpreted in one of two ways: (*a*) II at low concentrations actually increases the number of molecules bound to rat serum albumin, or (*b*) II does not change the number of sites available for interaction but, rather, changes the nature of the binding. Use of the electrochemical method permitted direct measurement of the amount of I free in solution. The early studies (10) were based on indirect spectrophotometric measurement. Ultrafiltration also provided direct measurement of free I.

In the electrochemical studies, the concentrations of I and rat serum albumin were twice those used by Witiak *et al.* (10), but the ratio of I to rat serum albumin was the same (1.07). Hence, the binding character also should be the same. Increasing the II concentration from 0 to 23.8×10^{-4} *M* produced the results shown in Fig. 5. The concentration of II used falls into the range where anomalous effects previously were observed spectrophotometrically. As shown in Fig. 5, identical results were obtained using the ultrafiltration technique. It is clear from this figure that II replaces I from its binding sites even at low concentrations. Therefore, it is apparent that II increases the ϵ^{477} for bound I at lower concentrations (10), and this increase is not a reflection of increased binding of I to rat serum albumin.

The reasons for this increase in ϵ^{477} may, as previously suggested, be due to a small molecular perturbation in rat serum albumin, which changes the I–rat serum albumin extinction coefficient, or to an interaction of bound I with closely bound II.

REFERENCES

(1) A. Goldstein, *Pharmacol. Rev.*, **1**, 102(1949).

(2) J. T. Edsall and J. Wyman, "Biophysical Chemistry," Academic, New York, N. Y., 1958, chap. 11, pp. 591–660.

(3) W. Scholtan, *Antibiot. Chemother.*, **12**, 103(1964).

(4) H. H. Stein, *Anal. Biochem.*, **13**, 305(1965).

(5) M. C. Meyer and D. E. Guttman, *J. Pharm. Sci.*, **57**, 1627 (1968).

(6) *Ibid.*, **59**, 33(1970).

(7) *Ibid.*, **59**, 39(1970).

(8) Y. W. Chien, C. L. Olson, and T. D. Sokoloski, *J. Pharm. Sci.*, **62**, 435(1973).

(9) M. Brezina and P. Zuman, "Polarography in Medicine, Biochemistry, and Pharmacy," Interscience, New York, N. Y., 1968.

(10) D. T. Witiak, T. D. Sokoloski, M. W. Whitehouse, and F. Hermann, *J. Med. Chem.*, **12**, 754(1969).

(11) D. T. Witiak, T. C.-L. Ho, R. E. Hackney, and W. E. Connor, *ibid.*, **11**, 1086(1968).

(12) G. Scatchard, *Ann. N. Y. Acad. Sci.*, **51**, 660(1949).

ACKNOWLEDGMENTS AND ADDRESSES

Received August 8, 1972, from the *College of Pharmacy, Ohio State University, Columbus, OH 43210*

Accepted for publication September 26, 1972.

Supported in part by Grants HL 12740 and GM 12998 from the National Institutes of Health, U. S. Public Health Service, Bethesda, MD 20014, and by Sterling-Winthrop Research Institute, Rensselaer, N. Y.

• Present address: Searle Laboratories, Chicago, IL 60680

▲ To whom inquiries should be directed.

Model Transport Studies Utilizing Lecithin Spherules III: Transport of Taurocholic Acid-[cholic-^{3}H(G)] in Buffered D-Glucose Solutions

ZAKA-UD-DIN T. CHOWHAN* and WILLIAM I. HIGUCHI▲

Abstract □ The transport of taurocholic acid-[cholic-^{3}H(G)] in liposome dispersions prepared from lecithin–dicetyl phosphate in buffered glucose solutions at different pH's was studied. The transport experiments were carried out using previously developed techniques in which the release of the solute is studied from dispersions contained in the dialysis bags. The experimental results of the direct-release and the uptake-release cases were analyzed by the monosize, multiconcentric layer Model 1 which was developed, evaluated, and used recently for D-glucose transport studies. Uniformly good fits of the experimental data with the model were observed, and the permeability coefficients and the aqueous–lipid partition coefficients for taurocholate transport in liposome dispersions were calculated. The pH dependence of the permeability coefficient indicated that the unionized form of taurocholic acid was being preferentially transported at low pH and that the taurocholate ion was the main species involved at high pH.

Keyphrases □ Permeability coefficients, taurocholic acid, radiolabeled—liposome dispersions □ D-Glucose solution—transport of taurocholic acid-[cholic-^{3}H(G)], lecithin spherule dispersions, permeability coefficients, pH effect □ Taurocholic acid, radiolabeled—transport in D-glucose solution, lecithin spherule dispersions, permeability coefficients, pH effect □ Lecithin spherules—model transport studies, taurocholic acid-[cholic-^{3}H(G)] in D-glucose solution, permeability coefficients □ Transport studies, model using lecithin spherules—taurocholic acid-[cholic-^{3}H(G)] in D-glucose solution, permeability coefficients, pH effect

In previous investigations (1, 2), quantitative methods were developed and used in the determination of permeability coefficients for D-glucose and 3-*O*-methyl-D-glucose in complex aqueous liposome dispersions. The release of the solutes from dispersions contained in a dialysis bag was studied as a function of time using

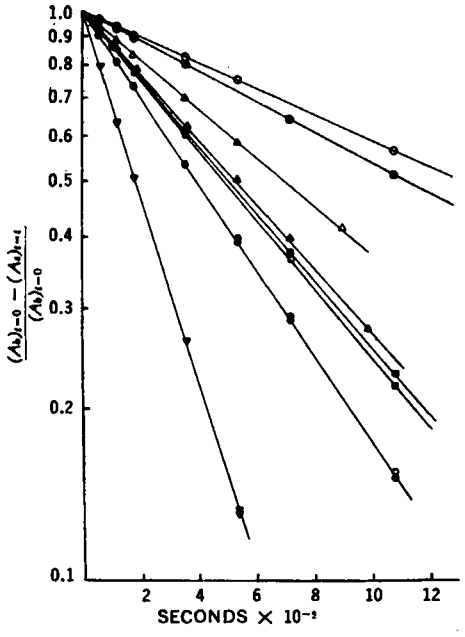

Figure 1—*First-order plots for determining the bag constants giving the transport of taurocholic acid and* D*-glucose through the dialysis bag membrane in buffered isotonic* (D*-glucose) solution. Key to transport of taurocholic acid:* ○, *0.01* M *acetate buffer at pH 3.6;* ●, *0.01* M *acetate buffer at pH 4;* △, *0.01* M *acetate buffer at pH 5;* ▲, *0.01* M *phosphate buffer at pH 7;* ■, *0.008* M *phosphate buffer at pH 8;* □, *0.01* M *phosphate buffer at pH 8;* ⬢, *0.01* M *phosphate buffer in 0.9% sodium chloride at pH 5; and* ○, *0.01* M *phosphate buffer in 0.9% sodium chloride at pH 7. Key to transport of* D*-glucose:* ▼, *0.01* M *acetate buffer at pH 5; and* ▽, *0.01* M *phosphate buffer at pH 7.*

direct-release and uptake-release experimental procedures. These data were analyzed using the monosize, multiconcentric layer models which assume that the spherules consist of multiconcentric bilayers of equal thickness separating aqueous compartments.

The purpose of the present investigation was to test the applicability of the previously developed techniques in the study of the transport behavior of an acidic compound, taurocholic acid. These studies were to be carried out under different pH conditions, and the influence of pH in altering the transport characteristics

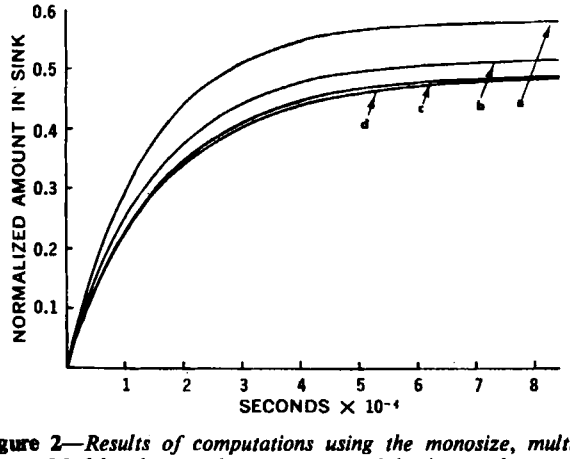

Figure 2—*Results of computations using the monosize, multiconcentric Model 1 showing the convergence of the direct-release curves. For curve a,* n = *5; for curve b,* n = *10; for curve c,* n = *20; and for curve d,* n = *30. Other parameter values are given in Table II under pH 7* (p = 2×10^{-10}).

Table I—Summary of the Parameter Values Determined at Different pH's for the Transport of Taurocholic Acid in Liposome Dispersions

pH	p	P	k_1	k_2
8 (0.01 *M* phosphate buffer)	1×10^{-9}	2.42×10^{-11}	34	140
8 (0.008 *M* phosphate buffer)	5×10^{-10}	1.21×10^{-11}	56	170
7 (0.01 *M* phosphate buffer)	5×10^{-10}	1.23×10^{-11}	50	260
5 (0.01 *M* acetate buffer)	1.5×10^{-9}	3.83×10^{-11}	82	290
4 (0.01 *M* acetate buffer)	4×10^{-8}	99.15×10^{-11}	95	345
3.6 (0.01 *M* acetate buffer)	8×10^{-8}	194.69×10^{-11}	210	600

of this solute was to be determined. It was hoped that the results of this study would help in the understanding of mechanisms that might be important in the movement of such molecules across biological membranes.

EXPERIMENTAL

General Considerations—The aqueous solution containing 5.1% anhydrous D-glucose was used earlier (1, 2) in the preparation of liposome dispersions. The same solution was used in the sink during a release run. Two reasons existed for the choice of this solution:

1. During the determination of the particle-size distribution by means of the Coulter counter, it was found important to make dilutions in 0.9% sodium chloride solution, which is isotonic, with the D-glucose solution used in the preparation of the dispersion.
2. It was not possible to prepare dispersions in 0.9% sodium chloride solution free from aggregates. Therefore, it was decided to conduct the present studies in buffered D-glucose solution at different pH's.

Materials—The procedures used in the purification of egg yolk lecithin were reported previously (1). Dicetyl phosphate[1] was used without further purification. Anhydrous D-glucose, potassium

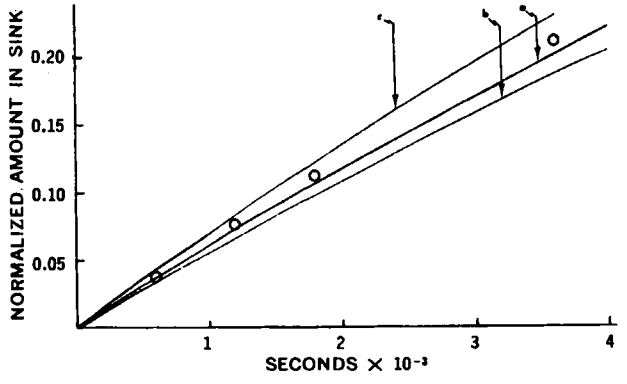

Figure 3—*Determination of* k_2 *from the initial data of the zero-hour uptake-release experiment for taurocholic acid from lecithin–dicetyl phosphate dispersions in buffered glucose solution at pH 7. Key:* ○, *experimental data. Curves represent calculation results. For curve a:* $k_1 = 48$, $k_2 = 260$, $p = 2 \times 10^{-10}$; $k_1 = 25$, $k_2 = 260$, $p = 2 \times 10^{-10}$; *and* $k_1 = 50$, $k_2 = 260$, $p = 5 \times 10^{-10}$. *For curve b:* $k_1 = 48$, $k_2 = 300$, $p = 2 \times 10^{-10}$. *For curve c:* $k_1 = 48$, $k_2 = 200$, $p = 2 \times 10^{-10}$.

[1] Sigma Chemical Co., St. Louis, Mo.

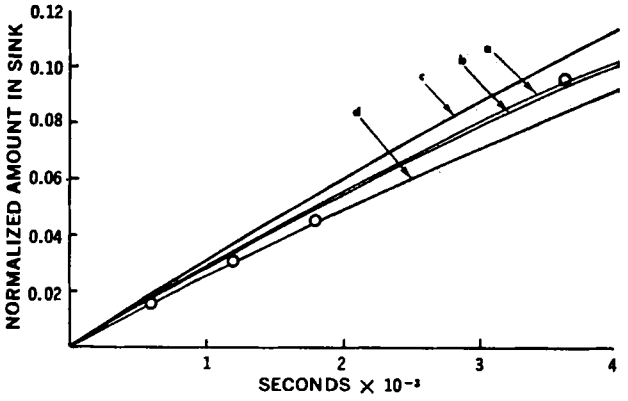

Figure 4—*Determination of* k_1 *from the initial data of direct-release experiment for taurocholic acid from lecithin–dicetyl phosphate dispersions in buffered glucose solution at pH 7. Key: O, experimental data. Curves represent computation results. For curve a:* $k_1 = 48$, $k_2 = 260$, $p = 2 \times 10^{-10}$. *For curve b:* $k_1 = 50$, $k_2 = 260$, $p = 2 \times 10^{-10}$; *and* $k_1 = 50$, $k_2 = 260$, $p = 5 \times 10^{-10}$. *For curve c:* $k_1 = 40$, $k_2 = 260$, $p = 2 \times 10^{-10}$. *For curve d:* $k_1 = 60$, $k_2 = 260$, $p = 2 \times 10^{-10}$.

phosphate monobasic and dibasic, sodium acetate, acetic acid, and chloroform were analytical reagent grade[2] and were used without further purification. Sodium chloride was also reagent grade[3] and used as such. The dialysis bags[4] were used without pretreatment. The water was double distilled in a glass apparatus. Taurocholic acid-[cholic-^{3}H(G)][5] was obtained in the form of methanol–ethanol (1:3) solution with a specific activity of 2–3 c./m*M*.

Apparatus and Procedures—The apparatus used for the taurocholic acid transport studies was exactly the same as reported previously (1). It consisted of a water-jacketed beaker and a dialysis bag holder–stirring assembly. Five milliliters of the dispersion was added to the dialysis bag, and at zero time the dialysis bag holder–stirring assembly was lowered into 100 ml. of sink solution maintained at 25°. The dispersion and the sink solution were stirred at 150 r.p.m. by two different stirring arrangements. At the end of each sampling time, the dialysis bag holder–stirring assembly was transferred to another water-jacketed beaker containing 100 ml. of fresh sink solution.

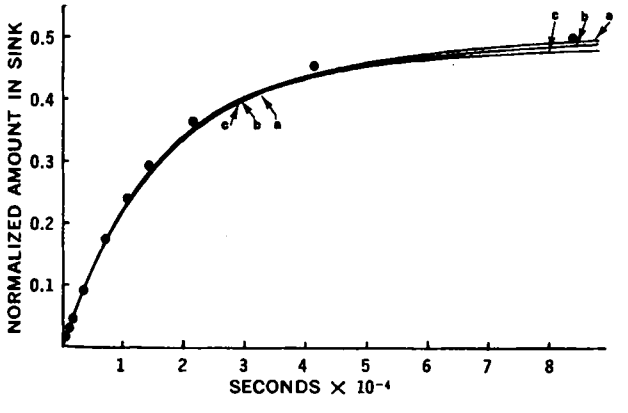

Figure 5—*Comparison of the direct-release experimental data obtained from lecithin–dicetyl phosphate dispersions for taurocholic acid released in 0.01* M *phosphate-buffered glucose solution at pH 7 with the calculations using the monosize, multiconcentric Model 1. Key: ●, experimental data. For curve a:* $k_1 = 50$, $k_2 = 260$, $p = 5 \times 10^{-10}$. *For curve b:* $k_1 = 48$, $k_2 = 260$, $p = 2 \times 10^{-10}$. *For curve c:* $k_1 = 50$, $k_2 = 260$, $p = 2 \times 10^{-10}$. *Other parameter values are taken from Table II.*

[2] J. T. Baker Chemical Co., Phillipsburg, N. J.
[3] Fisher Scientific Co., Fair Lawn, N. J.
[4] Union Carbide Corp., Chicago, Ill.
[5] New England Nuclear, Boston, Mass.

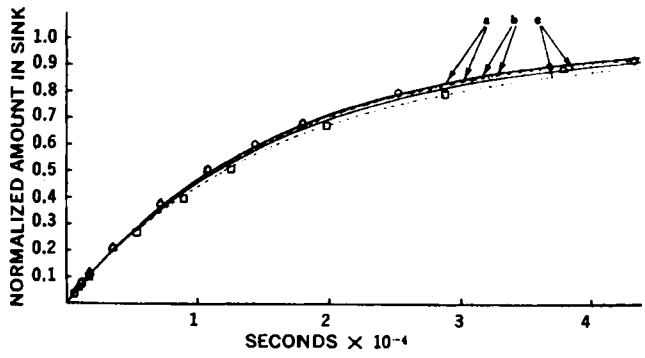

Figure 6—*Comparisons of the uptake-release experimental data obtained from lecithin–dicetyl phosphate dispersions for taurocholic acid release in 0.01* M *phosphate-buffered glucose solution at pH 7 with the calculations using the monosize, multiconcentric Model 1. Key (symbols represent experimental data): O, zero-hour solute uptake prior to release; Δ, 2-hr. solute uptake prior to release; and □, 10-hr. solute uptake prior to release. Curves a, b, and c represent calculations of 0-, 2-, and 10-hr. solute uptake, respectively. For solid curves:* $k_1 = 48$, $k_2 = 260$, $p = 2 \times 10^{-10}$; *and* $k_1 = 50$, $k_2 = 260$, $p = 2 \times 10^{-10}$. *For broken curves:* $k_1 = 50$, $k_2 = 260$, $p = 5 \times 10^{-10}$. *Other parameter values are taken from Table II.*

For the purpose of determining the bag constant (1, 2), the transport of the solute through the cellophane membrane was studied by the same procedure as used for the dispersion except that a buffered glucose solution containing the radioactive solute was used instead of the liposome dispersion.

The dispersions for the direct-release experiments were prepared (1) by mixing the chloroform solution of lecithin–dicetyl phosphate and the buffered glucose solution containing the radioactive solute. The solvent was then slowly removed using a flash evaporator with vacuum from a water aspirator. After the removal of chloroform, the dispersions were allowed to equilibrate for 2 hr. before starting the release run. The dispersions for the uptake-release experiments were prepared by the same procedure except that the radioactive solute was added to the dispersion after preparation.

The procedures for the determination of radioactive counts and for the Coulter counter particle-size distribution were the same as reported earlier (1).

THEORETICAL

Theoretical analyses carried out in the earlier reports (1, 2) indicated that the transport behavior of liposome dispersions could be quantitatively characterized by the physical models, assuming multiconcentric bilayers of lecithin separating aqueous compartments. The permeability coefficient per segment was related to the

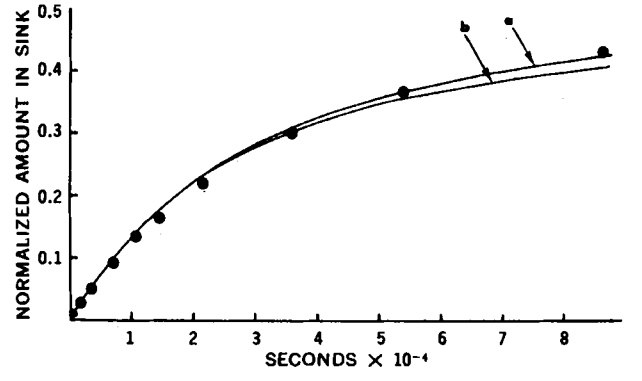

Figure 7—*Comparisons of the direct-release experimental data obtained from lecithin–dicetyl phosphate dispersions for taurocholic acid release in 0.01* M *acetate-buffered glucose solution at pH 5 with the calculations using the monosize, multiconcentric Model 1. Key: ●, experimental data. For curve a:* $k_1 = 82$, $k_2 = 290$, $p = 2.5 \times 10^{-9}$. *For curve b:* $k_1 = 82$, $k_2 = 290$, $p = 1.5 \times 10^{-10}$. *Other parameter values are taken from Table II.*

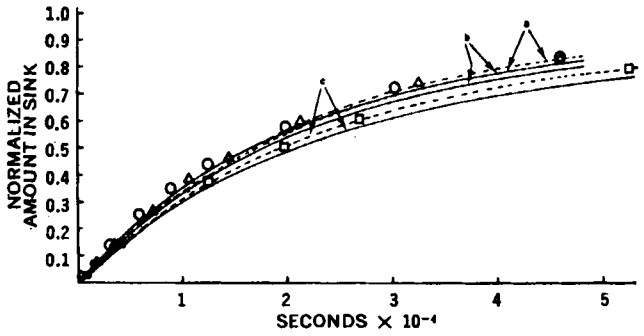

Figure 8—*Comparisons of the uptake-release experimental data obtained from lecithin–dicetyl phosphate dispersions for taurocholic acid release in 0.01* M *acetate-buffered glucose solution at pH 5 with the calculations using the monosize, multiconcentric Model 1. Key (symbols represent experimental data): ○, zero-hour solute uptake prior to release; △, 2-hr. solute uptake prior to release; and □, 10-hr. solute uptake prior to release. Curves a, b, and c represent calculations of 0-, 2-, and 10-hr. solute uptake, respectively. For solid curves:* $k_1 = 82$, $k_2 = 290$, $p = 2.5 \times 10^{-6}$. *For broken curves:* $k_1 = 82$, $k_2 = 290$, $p = 1.5 \times 10^{-6}$. *Other parameter values are taken from Table II.*

effective bulk permeability coefficient by the following equation:

$$p = \frac{P \cdot n}{r} \qquad \text{(Eq. 1)}$$

where p is the permeability coefficient per segment; n and r are the number of concentric layers and radius of the spherule, respectively; and P is the effective bulk permeability coefficient.

It was shown that the theoretical release curves converge at constant P as n is increased. On this basis it was proposed that the best P be determined at sufficiently large n.

Since the partition coefficients for D-glucose (1) and 3-*O*-methyl-D-glucose (2) were relatively small, the outermost lipid could be treated both as a part of the external phase (Model 1) and a part of the spherule (Model 2). Therefore, in the determination of permeability coefficients for 3-*O*-methyl-D-glucose, Model 2 was chosen for the data analysis.

Taurocholic acid transport studies indicated that relatively large amounts of solute bind to the lipid. Model 2, which was used for the transport studies of 3-*O*-methyl-D-glucose, failed to give reasonable agreements between the experiment and theory for this solute. Therefore, in the present studies the theoretical analyses were carried out using the monosize, multiconcentric layer Model 1. The equations describing Model 1 are given in the *Appendix* and were solved by means of a digital computer[6] as reported earlier (1).

RESULTS AND DISCUSSION

The results of the bag control experiments carried out in buffered glucose solutions at different pH's are presented in Fig. 1 in the form of semilogarithmic plots. The slopes of these first-order plots, from which the bag constants were determined (1), represent the bag constant divided by the volume inside the bag. At pH 5 and 7, when the glucose solution was replaced by 0.9% sodium chloride, the transport of taurocholic acid essentially followed the same rate. This indicated that the differences in the rate of taurocholic acid transport through the bag membrane at different pH's were mainly due to the differences in the ionic strength of the buffered glucose rather than to pH. Furthermore, the rate of D-glucose transport through the dialysis membrane remained unchanged in the same buffered glucose solution (pH 5 and 7) which gave significantly different slopes for taurocholate (Fig. 1).

The results of the zero-hour uptake-release experiments generally indicated a much greater binding of taurocholic acid with the outermost lipid layer compared with glucose and methyl glucose. Consequently, relatively large k_2 values were found (Table I). To study

[6] IBM 360.

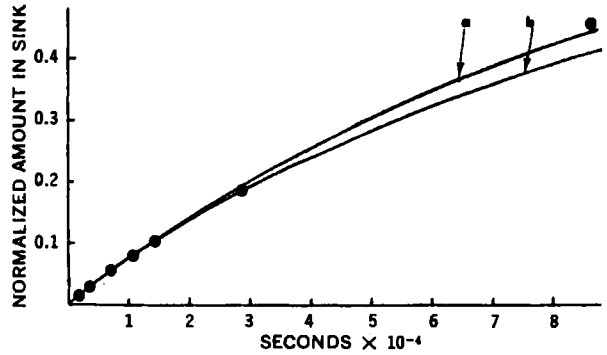

Figure 9—*Comparisons between the direct-release experimental data obtained from lecithin–dicetyl phosphate dispersions for taurocholic acid release in 0.01* M *acetate-buffered glucose solution at pH 4 and the calculations using the monosize, multiconcentric Model 1. Key: ●, experimental data. For curve a:* $k_1 = 120$, $k_2 = 345$, $p = 4 \times 10^{-6}$. *For curve b:* $k_1 = 120$, $k_2 = 260$, $p = 4 \times 10^{-6}$. *Other parameter values are taken from Table II.*

the convergence of the release curves when binding of the solute to the outermost lipid layer is much greater than binding in the inner lipid layers, it is important to keep the amount of solute bound to the last lipid layer constant. The convergence of the theoretical curves with respect to n of this system is typically illustrated by the results of computations given in Fig. 2 for the direct-release case. On the basis of these results, $n = 30$ was considered sufficiently large and was used throughout the present investigation.

The two partition coefficients k_1 and k_2 were determined from the initial rates of the direct-release and zero-hour uptake-release experiments. For a given n, the initial slope of the zero-hour uptake-release experiment is mainly a function of k_2. The determination of k_2 from the zero-hour uptake-release initial data for taurocholic acid in 0.01 M phosphate-buffered glucose solution at pH 7 is illustrated in Fig. 3. The calculations shown in Fig. 3 indicate that the initial slope of the zero-hour uptake-release experiment is insensitive to change in k_1 and p. The initial slope of the direct-release experiment is mainly a function of both k_1 and k_2. Once k_2 was determined, best k_1 values were determined by fitting the initial slope with the direct-release initial experimental points. The initial data of the direct-release experiment carried out in 0.01 M phosphate-buffered glucose solution at pH 7 are presented in Fig. 4. In this figure the theoretical curves show that the initial slope for this situation is insensitive to changes in p and is sensitive to k_1. The results of the direct-release and the uptake-release experiments

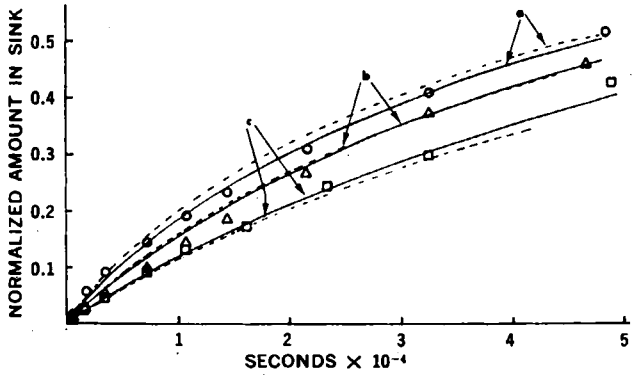

Figure 10—*Comparisons between the uptake-release experimental data obtained from lecithin–dicetyl phosphate dispersions for taurocholic acid release in 0.01* M *acetate-buffered glucose solution at pH 4 and the calculations using the monosize, multiconcentric Model 1. Key (symbols represent experimental data): ○, zero-hour solute uptake prior to release; △, 2-hr. solute uptake prior to release; and □, 10-hr. solute uptake prior to release. Curves a, b, and c represent calculations of 0-, 2-, and 10-hr. solute uptake, respectively. For solid curves:* $k_1 = 95$, $k_2 = 345$, $p = 4 \times 10^{-6}$. *For broken curves:* $k_1 = 120$, $k_2 = 260$, $p = 4 \times 10^{-6}$. *Other parameter values are taken from Table II.*

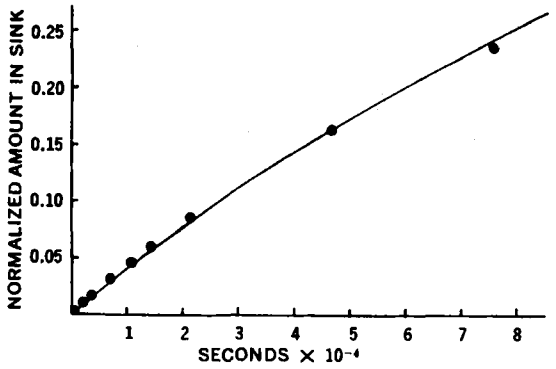

Figure 11—*Comparison between the direct-release experimental data obtained from lecithin–dicetyl phosphate dispersions for taurocholic acid release in 0.01* M *acetate-buffered glucose solution at pH 3.6 and the calculations using the monosize, multiconcentric Model 1. Key:* ●, *experimental data. Curve represents theory based on* $k_1 = 210$, $k_2 = 600$, $p = 8 \times 10^{-4}$, *and the parameter values given in Table II.*

carried out in buffered glucose solutions at different pH's for the transport of taurocholic acid are compared with the corresponding calculations in Figs. 5–12. The parameter values are given in Table II. As these data show, the uncertainty in the determination of the permeability coefficients becomes large when the permeability coefficients become very small. In spite of this limitation, the present results clearly show that the permeability coefficients are dependent on the pH of the media in which the taurocholic acid transport studies are performed.

In Fig. 13 the results of the direct-release experiments for the transport of D-glucose in buffered glucose solution (0.01 *M* acetate and phosphate) at different pH's are presented. The curve in this figure represents the results of computations carried out earlier (1) for the glucose transport studies in unbuffered glucose solution. The comparisons between the release data of D-glucose transport in buffered glucose solution at different pH's and the theoretical curve reproduced from the calculations for glucose transport in unbuffered glucose solution indicate no significant changes in the permeability coefficient of liposome membranes due to buffers or to changes in pH of the aqueous solution. This is a strong indication that the physical characteristics of the liposome membranes are not changed because of the changes in pH of the media, which is used for the preparation of dispersion and for the study of transport.

Since physical characteristics of the liposome dispersions do not seem to be significantly altered by changes in pH of the aqueous

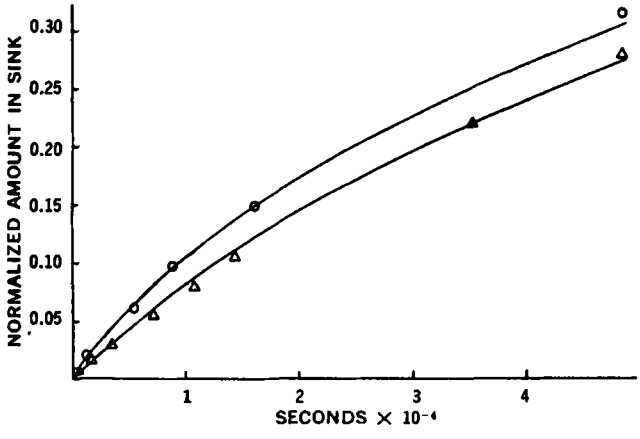

Figure 12—*Comparisons between the uptake-release experimental data obtained from lecithin–dicetyl phosphate dispersions for taurocholic acid release in 0.01* M *acetate-buffered glucose solution at pH 3.6 and the calculations using the monosize, multiconcentric Model 1. Key (symbols represent experimental data):* O, *zero-hour solute uptake prior to release; and* Δ, *2-hr. solute uptake prior to release. Corresponding curves represent calculations based on* $k_1 = 210$, $k_2 = 600$, $p = 8 \times 10^{-4}$, *and the parameter values given in Table I.*

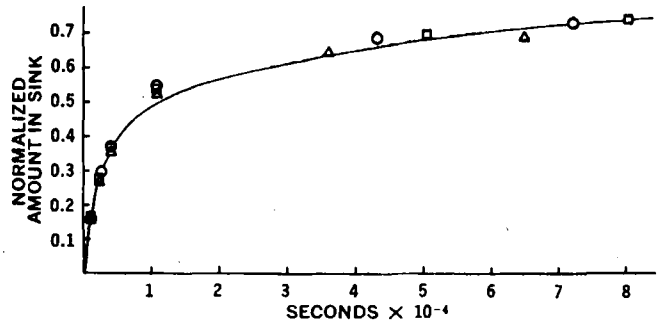

Figure 13—*Results showing little influence of pH for the release (direct release) of glucose from lecithin-dicetyl phosphate dispersion systems in buffered glucose solutions. Key:* O, *0.01* M *phosphate buffer at pH 8;* Δ, *0.01* M *phosphate buffer at pH 7; and* □, *0.01* M *acetate buffer.*

solution, it appears that the effect of pH is most likely related to the differences in the species of taurocholic acid in solution. The relationship between the effective bulk permeability coefficient and pH is given in Fig. 14. This relationship could be explained on the basis of the unionized form of taurocholic acid being preferentially transported. This would be in agreement with the pH-partition hypothesis of Shore *et al.* (3). The small, but finite, flux at high pH might be explained on the basis of the transport of the ionized species being the controlling factor under these conditions. This might have important implications in the *in vivo* absorption of taurocholate from bile.

APPENDIX

Monosize, multiconcentric layer models assume that all spherules are of the same size and consist of $i = 1$ to $i = n$ number of segments. In Model 1 the innermost aqueous phase is defined as segment 1. Segment 2 to segment n consists of an aqueous phase and a lipid phase which are of equal thickness. The outermost lipid phase is considered as a part of Compartment II, which is the external phase of the dispersion. In Model 2 the outermost lipid layer is considered as a part of the spherule so that each segment consists of an aqueous phase and a lipid phase. The basic assumptions, the equations, and the procedure used for solving these equations were reported earlier (1, 2). A summary of the equations used in Model 1 is presented here.

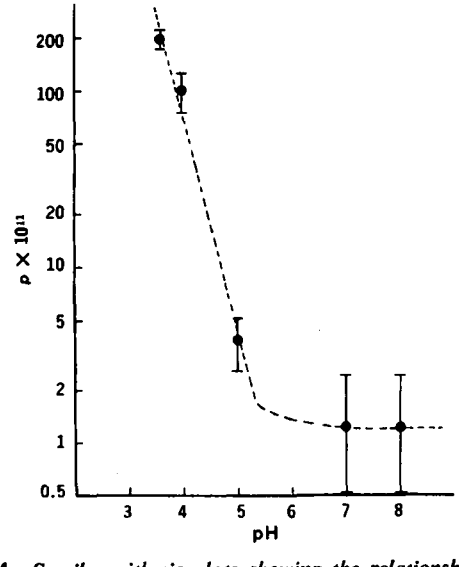

Figure 14—*Semilogarithmic plots showing the relationship between the effective bulk permeability coefficient for taurocholic acid and pH of the buffered glucose solution used in the preparation and in the release studies.*

Table II—Input Data Used in the Calculations Shown in Figs. 5–12 for the Taurocholic Acid Transport at Different pH's

pH	Volume of Spherules, ml.	Mean Surface Radius, μ	Number of Concentric Layers, n	Bag Constant $p_b \cdot S_b \times 10^4$, cm.^{3} sec.$^{-1}$	Permeability Coefficient per Segment, cm. sec.$^{-1}$
8 (0.01 *M* phosphate buffer)	0.922	0.725	30	7.023	1×10^{-9}
8 (0.008 *M* phosphate buffer)	0.922	0.725	30	6.790	5×10^{-10}
7 (0.01 *M* phosphate buffer)	0.930	0.738	30	6.483	5×10^{-10}
5 (0.01 *M* acetate buffer)	1.037	0.766	30	4.986	1.5×10^{-9}
4 (0.01 *M* acetate buffer)	0.973	0.744	30	3.272	4×10^{-8}
3.6 (0.01 *M* acetate buffer)	0.966	0.730	30	2.863	8×10^{-8}

The mass balance considerations for the $i = 2$ to the $i = n$ segment lead to Eq. A1:

$$(V_1 \cdot v_l + V_2 \cdot v_a)C_{2,t} = (V_1 \cdot v_l \cdot k_1 + V_2 \cdot v_a)C_{2,a}$$

$$\vdots$$

$$(V_{n-1} \cdot v_l + V_n \cdot v_a)C_{n,t} = (V_{n-1} \cdot v_l \cdot k_1 + V_n \cdot v_a)C_{n,a}$$

$$(V_n \cdot v_l + V_{II})C_{II,t} = (V_n \cdot v_l \cdot k_2 + V_{II})C_{II,a} \quad \text{(Eq. A1)}$$

where:

$V_1 \ldots V_n$ = volume of segment 1 to segment n
V_{II} = volume of Compartment II (external phase of the dispersion)
v_l = volume fraction of lipid phase
v_a = volume fraction of aqueous phase
$C_2 \ldots C_n$ = average solute concentration of segment 2 to segment n
$C_{II,t}$ = average solute concentration of Compartment II
$C_{2,a} \ldots C_{n,a}$ = aqueous solute concentration of segment 2 to segment n
$C_{II,a}$ = aqueous solute concentration in Compartment II
k_1 = effective lipid–aqueous partition coefficient that applies to the lipid and aqueous phases in the $i = 2$ to $i = n$ segments
k_2 = effective lipid–aqueous partition coefficient that applies to the outermost lipid phase and Compartment II

The rates at which solute leaves segments $i = 1$ to $i = n$ are given by Eq. A2:

$$-V_1 \cdot v_a \cdot \frac{dC_{1,a}}{dt} = S_1 \cdot p(C_{1,a} - C_{2,a})$$

$$(V_1 \cdot v_l \cdot k_1 + V_2 \cdot v_a)\frac{dC_{2,a}}{dt} = S_1 \cdot p(C_{1,a} - C_{2,a}) - S_2 \cdot p(C_{2,a} - C_{3,a})$$

$$\vdots$$

$$(V_{n-1} \cdot v_l \cdot k_1 + V_n \cdot v_a)\frac{dC_{n,a}}{dt} = S_{n-1} \cdot p(C_{n-1,a} - C_{n,a}) - S_n \cdot p(C_{n,a} - C_{II,a}) \quad \text{(Eq. A2)}$$

where:

$S_1 \ldots S_n$ = surface area of segment 1 to segment n
p = permeability coefficient per segment

The rate of appearance of solute in Compartment II is given by Eq. A3:

$$(V_n \cdot v_l \cdot k_2 + V_{II})\frac{dC_{II,a}}{dt} = S_n \cdot p(C_{n,a} - C_{II,a}) - S_b \cdot p_b \cdot C_{II,a} \quad \text{(Eq. A3)}$$

where:

S_b = surface area of dialysis membrane
p_b = effective permeability coefficient of bag

The rate of appearance of solute in the sink is given by Eq. A4:

$$\frac{dAs}{dt} = p_b \cdot S_b \cdot C_{II,a} \quad \text{(Eq. A4)}$$

where As = the amount of solute in the sink normalized with respect to the initial amount in the bag.

REFERENCES

(1) Z. T. Chowhan, T. Yotsuyanagi, and W. I. Higuchi, *Biochim. Biophys. Acta*, **266**, 320(1972).

(2) Z. T. Chowhan, T. Yotsuyanagi, and W. I. Higuchi, *J. Pharm. Sci.*, **62**, 221(1973).

(3) P. A. Shore, B. B. Brodie, and C. A. M. Hogben, *J. Pharmacol. Exp. Ther.*, **119**, 361(1957).

ACKNOWLEDGMENTS AND ADDRESSES

Received June 9, 1972, from the *College of Pharmacy, University of Michigan, Ann Arbor, MI 48104*

Accepted for publication October 4, 1972.

Supported by National Institute of Dental Research Training Grant DE-00204 and by National Institute of General Medical Sciences Grant GM-13368.

* Present address: Institute of Pharmaceutical Sciences, Syntex Corporation, Stanford Industrial Park, Palo Alto, CA 94304

▲ To whom inquiries should be directed.